Regulation of the NKCC2 ion cotransporter by SPAK-OSR1-dependent and -independent pathways

Ciaran Richardson[1,*], Kei Sakamoto[1], Paola de los Heros[1], Maria Deak[1], David G. Campbell[1], Alan R. Prescott[2] and Dario R. Alessi[1,*]

[1]MRC Protein Phosphorylation Unit, College of Life Sciences, University of Dundee, Dow Street, Dundee DD1 5EH, UK
[2]Division of Cell Signalling and Immunology, College of Life Sciences, University of Dundee, Dow Street, Dundee DD1 5EH, UK
*Authors for correspondence (d.r.alessi@dundee.ac.uk; c.j.z.richardson@dundee.ac.uk)

Accepted 20 October 2010
Journal of Cell Science 124, 789-800

doi:10.1242/jcs.077230

Summary

Ion cotransporters, such as the Na^+/Cl^- cotransporter (NCC), control renal salt re-absorption and are regulated by the WNK-signalling pathway, which is over-stimulated in patients suffering from Gordon's hypertension syndrome. Here, we study the regulation of the NKCC2 (SLC12A1) ion cotransporter that contributes towards ~25% of renal salt re-absorption and is inhibited by loop-diuretic hypertensive drugs. We demonstrate that hypotonic low-chloride conditions that activate the WNK1-SPAK and OSR1 pathway promote phosphorylation of NKCC2 isoforms (A, B and F) at five residues (Ser91, Thr95, Thr100, Thr105 and Ser130). We establish that the SPAK and OSR1 kinases activated by WNK interact with an RFQV motif on NKCC2 and directly phosphorylate Thr95, Thr100, Thr105 and, possibly, Ser91. Our data indicate that a SPAK-OSR1-independent kinase, perhaps AMP-activated protein kinase (AMPK), phosphorylates Ser130 and that phosphorylation of Thr105 and Ser130 plays the most important roles in stimulating NKCC2 activity. In contrast with NCC, whose membrane translocation is triggered by SPAK-OSR1 phosphorylation, NKCC2 appears to be constitutively at the membrane. Our findings provide new insights into how NKCC2 is regulated and suggest that inhibitors of SPAK and/or OSR1 for the treatment of hypertension would be therapeutically distinct from thiazide or loop diuretics, as they would suppress the activity of both NCC and NKCC2.

Key words: AMPK, Blood pressure, NCC, NKCC2, SPAK-OSR1, WNK

Introduction

SPAK (for 'STE20-and-SPS1-related proline and alanine-rich kinase') and OSR1 (oxidative-stress-responsive kinase 1) are related members of the STE20 kinase subfamily and are activated by the WNK1 [with-no-K(Lys) kinase 1] and WNK4 protein kinases (Anselmo et al., 2006; Moriguchi et al., 2005; Vitari et al., 2005). The genes encoding WNK1 and WNK4 are mutated in patients suffering from pseudo-hypoaldosteronism type II (PHAII), an inherited hypertension and hyperkalaemia (elevated plasma K^+) disorder also known as Gordon's syndrome (Wilson et al., 2001). WNK1 activates SPAK and OSR1 by phosphorylating a Thr residue (SPAK Thr233, OSR1 Thr185) within their T-loop (Vitari et al., 2005). WNK1 also phosphorylates SPAK and OSR1 at a Ser residue within their S-motif (SPAK Ser373, OSR1 Ser325); however, the role that this phosphorylation plays is unknown, as mutation of this residue does not affect activation of SPAK-OSR1 (Vitari et al., 2005; Zagorska et al., 2007). WNK isoforms, and hence SPAK-OSR1, are activated rapidly following hypertonic or hypotonic low-chloride conditions (Anselmo et al., 2006; Lenertz et al., 2005; Moriguchi et al., 2005; Richardson et al., 2008; Zagorska et al., 2007). The best-characterised substrates of SPAK and OSR1 are the $Na^+/K^+/2Cl^-$ ion cotransporter NKCC1 (SLC12A2) (Dowd and Forbush, 2003; Piechotta et al., 2002) and the thiazide-sensitive Na^+/Cl^- ion cotransporter (NCC) (Flatman, 2008; Gamba, 2005; Richardson and Alessi, 2008). These ion cotransporters are members of the Na^+-driven branch of SLC12 ion cotransporters, which are highly glycosylated enzymes possessing 12 transmembrane regions flanked by regulatory N-terminal and C-terminal cytoplasmic domains (Gamba, 2005).

NKCC1 is ubiquitously expressed and plays vital roles in regulating cellular ion homeostasis and protection from osmotic shock (Flatman, 2008). By contrast, NCC is exclusively expressed in the distal convoluted tubule in the kidney and regulates renal salt re-absorption and, thereby, blood pressure. Thiazide diuretics are deployed as frontline treatments for hypertension and exert their effects by promoting salt excretion from the body by inhibiting the activity of NCC (O'Shaughnessy and Karet, 2006; Simon et al., 1996b). Loss of function mutations in NCC in humans results in the low blood pressure Gitelman's syndrome (Simon et al., 1996b). SPAK and OSR1 interact with NKCC1 and NCC through a unique CCT (conserved C-terminal) docking domain that interacts with RFXV/I motifs at the N-terminal domain of NKCC1 (Gagnon et al., 2007) and NCC (Richardson et al., 2008). SPAK and OSR1 activate NKCC1 and NCC by phosphorylating a cluster of conserved Thr residues in the N-terminal cytosolic domain of NKCC1 and NCC that we have termed sites 1 to 4 (Fig. 1A). Consistent with this, osmotic stress that induces activation of the WNK pathway leads to phosphorylation of NKCC1 and NCC in vivo at the residues that SPAK and/or OSR1 phosphorylate in vitro (Richardson et al., 2008; Vitari et al., 2006). Furthermore, mutation of key SPAK-OSR1 phosphorylation sites on NKCC1 (Thr217, human) (Darman and Forbush, 2002; Gagnon et al., 2007) or on NCC (Thr60, human) (Pacheco-Alvarez et al., 2006; Richardson et al., 2008) prevents osmotic-stress-induced activation of these ion transporters. Knock-in mice expressing a form of SPAK that cannot be activated by WNK isoforms have low blood pressure and reduced phosphorylation of NCC, as well as NKCC1, in the kidney (Rafiqi et al., 2010). Moreover, a Thr60Met missense mutation

that ablates the key SPAK-OSR1 phosphorylation site in NCC is frequently detected in Asian patients with Gitelman's syndrome (Lin et al., 2005; Maki et al., 2004; Shao et al., 2008).

A third pivotal SLC12 ion cotransporter family member is the $Na^+/K^+/2Cl^-$ ion cotransporter NKCC2 (SLC12A1). NKCC2 is exclusively expressed in the apical membrane of the thick ascending limb of the kidney (Flatman, 2008; Gamba, 2005). NKCC2 is estimated to contribute to 20–25% of all renal salt re-absorption, i.e. more than NCC, which contributes 5–10% (O'Shaughnessy and Karet, 2006). NKKC2 is inhibited by loop diuretics, and loss-of-function mutations of NKCC2 in humans result in the low blood pressure Bartter's type I syndrome, which is more severe than the loss-of-function NCC Gitelman's syndrome (Simon et al., 1996a; Simon et al., 1996b). Differential spicing of exon four of NKCC2 results in three variants termed isoform F, isoform A and isoform B (Payne and Forbush, 1994), which vary in amino acid sequence in a region of the protein that encodes for the predicted second transmembrane domain and part of the following first intracellular loop (Fig. 1B). These isoforms differ in their transcript levels, localisation and ion affinity properties (Castrop and Schnermann, 2008).

Sequence alignments indicate that the cluster of residues on NCC and NKCC1 that are phosphorylated by SPAK-OSR1 are conserved on NKCC2 (Fig. 1A). SPAK and OSR1 were shown to phosphorylate an N-terminal fragment of NKCC2 in vitro, but the phosphorylation sites were not mapped (Moriguchi et al., 2005). A recent study has also demonstrated that overexpression of WNK3 in *Xenopus laevis* oocytes leads to activation of NKCC2 in a manner that is dependent upon the interaction of SPAK-OSR1 with WNK3 (Ponce-Coria et al., 2008). Furthermore, in a *Xenopus laevis* oocyte overexpression system, mutation of the NKCC2 Thr residue equivalent to Thr60 in NCC (human NKCC2 Thr105) inhibited activity (Gimenez and Forbush, 2005; Ponce-Coria et al., 2008). In this study, we sought to characterise in more detail the mechanism by which NKCC2 is regulated by SPAK and OSR1 in a mammalian system. Our findings provide further molecular insights into how NKCC2 is regulated by the WNK-SPAK-OSR1 signalling pathway and indicate that disruptions in the WNK signalling network will impact upon blood pressure through NCC as well as NKCC2. Inhibitors of SPAK-OSR1 for the treatment of hypertension would thus be distinct from thiazide or loop diuretics as they would suppress activity of both NCC and NKCC2.

Results

SPAK and OSR1 phosphorylate NKCC2 at Thr95 and Thr100 in vitro

We first verified that activated SPAK or OSR1 phosphorylated a fragment of human NKCC2 (residues 1–174) encompassing the N-terminal cytoplasmic domain (supplementary material Fig. S1A,B). A constitutively active mutant of SPAK-OSR1, in which the T-loop Thr residue phosphorylated by WNK1 was mutated to Glu in order to mimic phosphorylation, was employed in these in vitro phosphorylation studies. NKCC2(1–174) was phosphorylated by activated SPAK or OSR1 to a stoichiometry of ~0.3 and ~0.7 mol of phosphate per mol of NKCC2(1–174), respectively. Catalytically inactive mutants of SPAK or OSR1 did not phosphorylate NKCC2(1–174) (supplementary material Fig. S1A). [^{32}P]NKCC2(1–174) phosphorylated by activated SPAK was digested with trypsin and chromatographed on a C18 column to isolate ^{32}P-labelled phosphorylated peptides. This revealed two sharp peaks (P1 and P3) and a broader peak that we subdivided

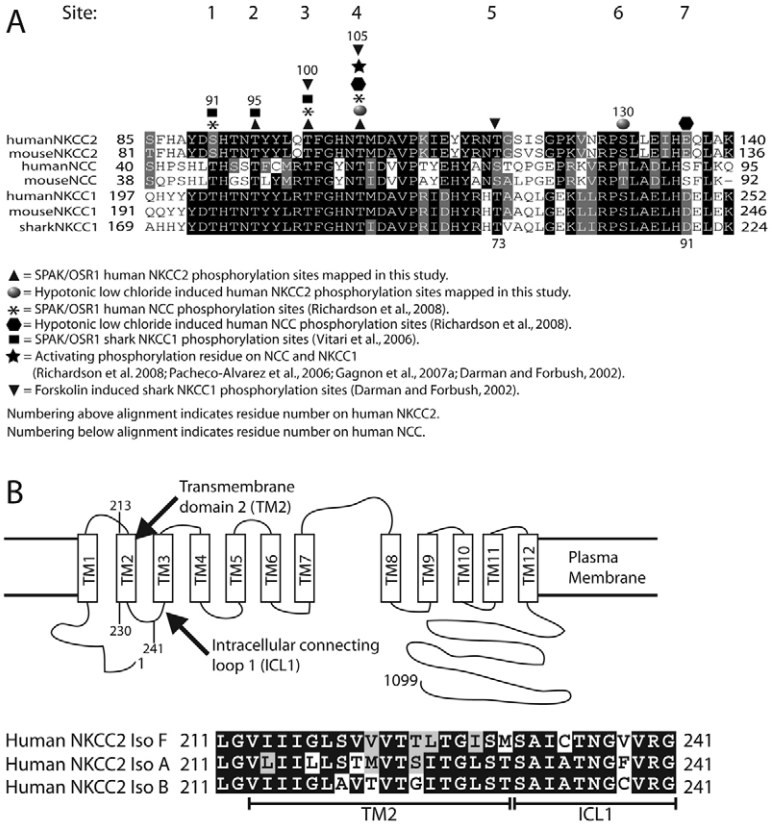

Fig. 1. Schematics of the NCC and NKCC proteins. (**A**) Sequence alignment of the N-terminal region of SLC12 electroneutral cation-chloride-coupled cotransporters that are regulated by phosphorylation. Identical residues are highlighted in black and similar residues are in grey. Symbols indicate characterised phosphorylation sites, and the seven phosphorylation sites of interest discussed in this study are numbered from 1 to 7. (**B**) Alternative splicing of exon four results in three isoforms of NKCC2 (isoform F, isoform A and isoform B). The predicted domain structure of NKCC2 is shown and the region of NKCC2 encoded by the alternatively spliced exons is indicated (the second transmembrane domain and the first part of the first intracellular connecting loop). The sequence differences between the NKCC2 isoforms arising from alternative splicing of exon four are illustrated in the sequence alignment. Identical residues are highlighted in black and similar residues are in grey.

into two fractions (P2a and P2b) (supplementary material Fig. S1C). Mass spectrometry, solid-phase Edman sequencing and mutational analysis established the identity of peptides P2a and P3 as tryptic peptides phosphorylated at Thr95 (supplementary material Fig. S1D,E). Peptides P1 and P2b encompassed tryptic peptides phosphorylated at Thr100 (supplementary material Fig. S1D,E). [^{32}P]NKCC2(1–174) phosphorylated by activated OSR1 was analysed in a similar fashion, and Thr95 and Thr100 were also identified as the major in vitro phosphorylation sites (supplementary material Fig. S2). Mutation of Thr95 did not markedly reduce phosphorylation of NKCC2(1–174) by either SPAK or OSR1 (supplementary material Fig. S1F). Mutation of Thr100 reduced phosphorylation of NKCC2(1–174) by either SPAK or OSR1 ~60%, whereas combined mutation of both Thr95 and Thr100 virtually abolished phosphorylation (supplementary material Fig. S1F), confirming that Thr95 and Thr100 comprise the major in vitro phosphorylation sites.

Hypotonic low-chloride conditions induce phosphorylation of NKCC2 in HEK-293 cells at five residues

To map the in vivo sites of phosphorylation on NKCC2, we undertook mass spectrometry phosphorylation-site-mapping analysis of NKCC2 isoform F overexpressed in HEK-293 cells treated with either basic control medium or hypotonic low-chloride medium that activates the WNK-SPAK-OSR1 signalling pathway. NKCC2 isoform F was selected for this analysis as it had previously been reported to be the most abundant NKCC2 isoform in mouse kidney (Castrop and Schnermann, 2008), although a recent study has suggested that NKCC2 isoform A might be the dominant isoform in human kidney (Carota et al., 2010). Hypotonic low-chloride conditions activated the WNK1-SPAK-OSR1-signalling pathway, as demonstrated by increased phosphorylation of WNK1(Ser382) and SPAK-OSR1 (Thr233 or Thr185, respectively) at their T-loop activation residues (Fig. 2A). NKCC2 was immunoprecipitated from cells under control and hypotonic low-chloride conditions (Fig. 2B), digested with trypsin and the resulting peptides were subjected to phosphorylated peptide identification analysis by LC–MS (liquid chromatography–mass spectrometry) with an Orbitrap and precursor ion scanning on a Q-trap mass spectrometer. This revealed that hypotonic low-chloride conditions, in addition to inducing phosphorylation of NKCC2 at a peptide encompassing Thr95 and Thr100, also promoted marked phosphorylation of two other residues, namely Thr105 and Ser130 (Fig. 2C).

We next generated phosphorylation-specific antibodies against the four identified NKCC2 phosphorylation sites (Thr95, Thr100, Thr105 and Ser130). We also raised a fifth phosphorylation-specific antibody against Ser91 of human NKCC2, which was not identified in the above studies, because of the fact that the equivalent Thr residue in both NKCC1 (human Thr203) and NCC (human Thr46) is phosphorylated by SPAK-OSR1 (Richardson et al., 2008; Vitari et al., 2006) (Fig. 1A). Of the five antibodies generated, antibodies against Ser91, Thr105 and Ser130 were specific, as mutation of these residues to Ala prevented recognition (Fig. 3A). Although we were unsuccessful in raising NKCC2 Thr95 and Thr100 phosphorylation-specific antibodies (data not shown), we found that an antibody that detected the equivalent residue of phosphorylated NCC (human Thr55) (Richardson et al., 2008) recognised NKCC2 phosphorylated at Thr100 (Fig. 3A). Using these phosphorylation-specific antibodies we establish that hypotonic low-chloride stimulation induces marked phosphorylation of overexpressed NKCC2 in HEK-293 cells at Ser91, Thr100, Thr105 and Ser130 (Fig. 3A).

SPAK-OSR1 does not phosphorylate NKCC2 at Ser130 in vitro

As the in vitro phosphorylation of NKCC2(1–174) by SPAK-OSR1 (supplementary material Figs S1 and S2) did not identify phosphorylation of Ser91, Thr105 or Ser130, possibly owing to low stoichiometry of phosphorylation of the bacterially expressed NKCC2(1–174) at these sites, we re-analysed the in vitro phosphorylation reactions employing the more sensitive phosphorylation-specific antibodies. This confirmed that SPAK-OSR1 phosphorylated Thr100 and also revealed detectable levels of Thr105 phosphorylation. However, we did not observe any phosphorylation of Ser91 and Ser130 in these experiments. Mutation of Ser130, but not the other residues tested, moderately diminished the in vitro phosphorylation of NKCC2 by SPAK and OSR1 at Thr105 (Fig. 3B). Mutation of Ser130 also modestly

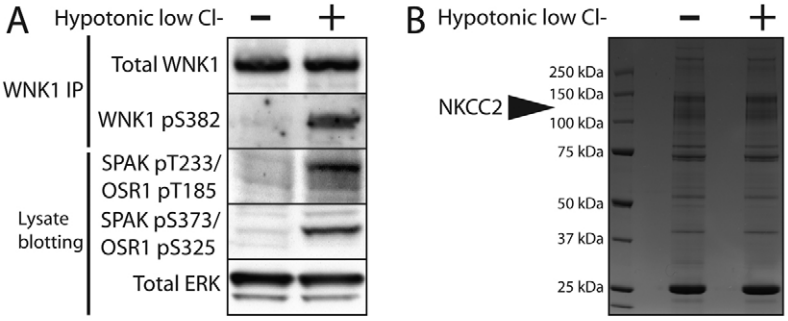

C

Peptide ID	m/z	Number of Phosphates	Site of Phosphorylation on Peptide	Basic buffer	Hypotonic low Cl- buffer
VNRP(p)SLLEIHEQLAK	609.7	1	Ser130	Phospho-peptide absent	Phospho-peptide detected
TDASFHAYDSHTNTYYLQ TFGHN(p)TmDAVPK	882.9	1	Thr105	Phospho-peptide absent	Phospho-peptide detected
TDASFHAYDSHTNTYYLQ TFGHNTmDAVPK	1203.5	2	Thr95/Thr100?	Phospho-peptide absent	Phospho-peptide detected

Fig. 2. Identification of in vivo phosphorylation sites on NKCC2 following activation of the WNK1-SPAK-OSR1 signalling cascade. (**A**) HEK-293 cells were transfected with a construct expressing human FLAG–NKCC2 (isoform F) and, at 36 hours post-transfection, the cells were treated with either basic (–) or hypotonic low-chloride medium (+) for 30 minutes. Endogenous WNK1 was immunoprecipitated (IP) and immunoblotted for the indicated proteins. Total cell lysates were also immunoblotted for the indicated proteins. (**B**) FLAG–NKCC2 was immunoprecipitated, electrophoresed on a polyacrylamide gel and stained with Colloidal Blue. (**C**) The Colloidal-Blue-stained bands corresponding to FLAG–NKCC2 were excised and digested with trypsin. Phosphorylated peptides were identified by combined liquid chromatography–mass spectrometry and tandem mass spectrometry analysis. The table outlines peptides whose phosphorylation was increased by the hypotonic low-chloride conditions. The deduced amino acid sequence of each peptide is shown and the phosphorylated residue where identified is preceded by (p). The 'm' in peptide sequence indicates methionine sulphoxide; *m/z*, atomic mass units (amu).

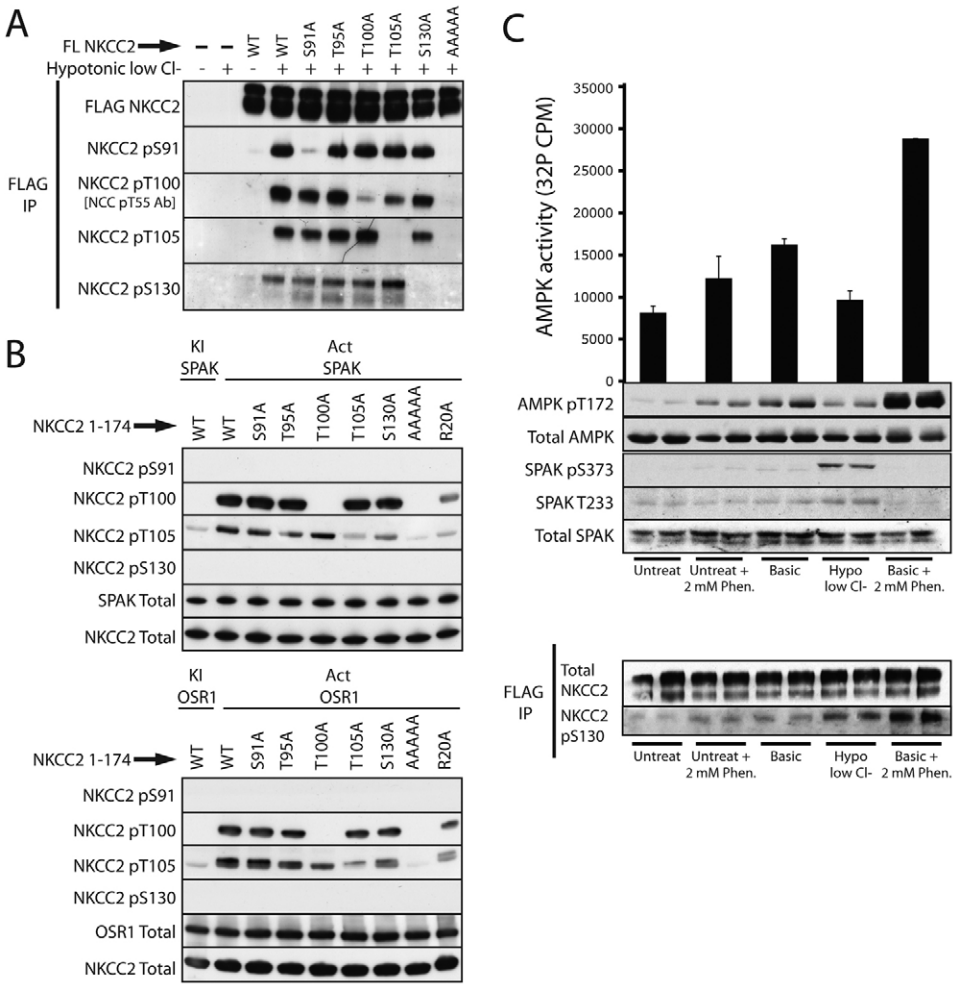

Fig. 3. NKCC2 phosphorylation-site characterisation employing phosphorylation-specific antibodies. (**A**) HEK-293 cells were transfected with constructs encoding the wild-type (WT) or the indicated mutant forms of human FLAG–NKCC2 (isoform F). At 36 hours post-transfection, cells were treated with either basic (–) or hypotonic low-chloride (+) medium for 30 minutes and lysed. FLAG–NKCC2 was immunoprecipitated (IP) and immunoblotted with NKCC2 phosphorylation-specific and total antibodies. Similar results were obtained in two separate experiments. AAAAA corresponds to a quintuple NKCC2(1–174) mutant in which Ser91, Thr95, Thr100, Thr105 and Ser130 are replaced with Ala. (**B**) Wild-type or the indicated mutants of GST–NKCC2(1–174) were phosphorylated with active (Act) or kinase-inactive (KI) mutants of GST–SPAK or GST–OSR1 and the phosphorylation was analysed by immunoblotting. The employed kinase-inactive and active mutants of SPAK and OSR1 are described fully in the legend to supplementary material Fig. S1A. (**C**) Stably transfected HEK-293 T-Rex cells were induced to express wild-type human FLAG–NKCC2 (isoform F). At 24 hours post-induction, cells were left in DMEM (Untreat) or treated with basic buffer for 30 minutes, hypotonic low-chloride buffer for 30 minutes, or basic buffer in the presence (+) of 2 mM phenformin (AMPK activator) for 60 minutes and lysed. Endogenous AMPKα1 was immunoprecipitated and its activity assayed by employing the AMARA peptide substrate. The incorporation of ^{32}P-radioactivity was quantified and the results are presented as the mean activity (±s.d.) for triplicate samples. Total cell extracts were immunoblotted with for the indicated proteins and NKCC2 Ser130 phosphorylation was monitored by immunoblotting following immunoprecipitation of FLAG–NKCC2. Similar results were obtained in two separate experiments.

diminished the phosphorylation of NKCC2 at Thr105 in cells in hypotonic low-chloride conditions (Fig. 3A).

Hypotonic low-chloride-induced NKCC2 Ser130 phosphorylation is potentially mediated by AMPK

Recent work has reported that the AMP-activated protein kinase (AMPK) could phosphorylate Ser130 on NKCC2 (Cook et al., 2009; Fraser et al., 2007). To investigate the role of AMPK in regulating phosphorylation of NKCC2 at Ser130, cells stably expressing the NKCC2 isoform F were treated with basic buffer, hypotonic low-chloride buffer or basic buffer containing the AMPK activator phenformin. As an additional control, cells were left in Dulbecco's modified Eagle's medium (DMEM) with or without phenformin (untreated, Fig. 3C). As expected, phenformin robustly stimulated the T-loop phosphorylation (Thr172) of AMPK, leading to enhanced AMPK activity (Fig. 3C) in both untreated and basic buffer conditions. Consistent with AMPK phosphorylating NKCC2 at Ser130, phenformin also induced phosphorylation of NKCC2 at Ser130. However, hypotonic low-chloride conditions did not stimulate Thr172 phosphorylation or activate AMPK but still led to phosphorylation of NKCC2 at Ser130, although to a lower extent than observed with phenformin (Fig. 3C). This would suggest that under these conditions AMPK is not mediating phosphorylation of Ser130. To investigate further the role of AMPK in regulating Ser130 phosphorylation, we employed the non-selective inhibitor of AMPK compound C (Zhou et al., 2001). We found that

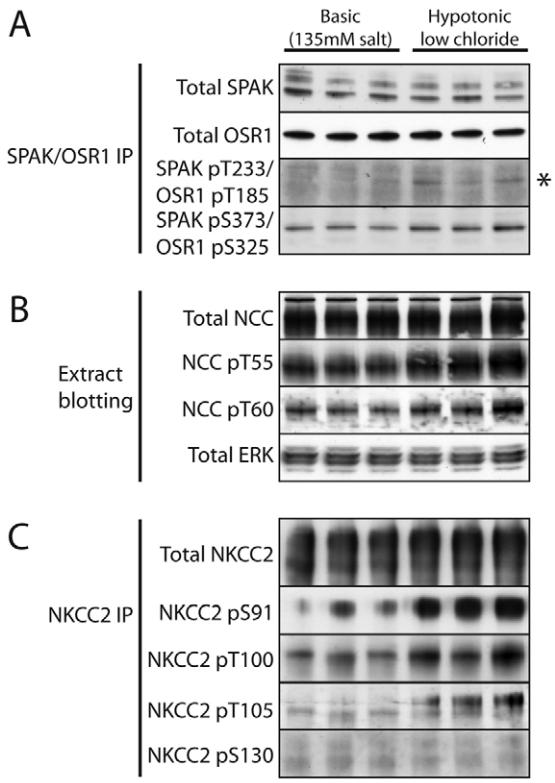

Fig. 4. Endogenous NKCC2 phosphorylation in perfused mouse kidney extracts. (**A**) Mouse kidneys were perfused for 15 minutes with basic or hypotonic low-chloride buffers as described in the Materials and Methods section. SPAK and OSR1 were immunoprecipitated (IP) from the perfused mouse kidney extracts by employing a biotinylated RFQV motif-containing peptide and the immunoprecipitates were subjected to immunoblot analysis with total and phosphorylation-specific antibodies against the indicated proteins. (**B**) Perfused mouse kidney extracts were immunoblotted with total and phosphorylation-specific antibodies against the indicated NCC proteins. Mouse perfusion experiments were performed with three animals and similar results were obtained in two separate experiments. (**C**) NKCC2 was immunoprecipitated from perfused mouse kidney extracts and immunoblotted with total and phosphorylation-specific antibodies against the indicated NKCC2 proteins.

compound C partially diminished AMPK activity in cells treated with hypotonic low-chloride buffer and phenformin as judged by diminished phosphorylation of the downstream substrate of AMPK, raptor (supplementary material Fig. S3). NKCC2 Ser130 phosphorylation was also diminished to a similar extent as raptor phosphorylation in cells treated with compound C (supplementary material Fig. S3). Although this suggests that AMPK could be the NKCC2 Ser130 kinase that is active under hypotonic low-chloride conditions, as compound C is not very selective, it is possible that it is exerting its effect by inhibiting another kinase (Bain et al., 2007).

Phosphorylation of endogenous NKCC2 in mouse kidney

To study phosphorylation of endogenous NKCC2, we first screened a number of renal cell lines, including inner medullar collecting duct (mpkIMCD) (Van Huyen et al., 2001), cortical collecting duct (mpkCCD) (Van Huyen et al., 2001) and mouse macula-densa-derived-1 (MMDD1) (Yang et al., 2000) cells. As none of these cells expressed detectable levels of endogenous NKCC2, we monitored endogenous NKCC2 phosphorylation following perfusion of mouse kidneys with basic or hypotonic low-chloride solutions. Perfusion of mouse kidney with hypotonic low-chloride conditions activated SPAK-OSR1 as judged by increased phosphorylation of the T-loop and S-motif residues on SPAK-OSR1 phosphorylated by WNK isoforms (Fig. 4A), as well as by increased phosphorylation of NCC at the SPAK-OSR1 phosphorylation sites (Fig. 4B). NKCC2 was immunoprecipitated from whole-kidney extracts and subjected to immunoblotting with total and phosphorylation-specific NKCC2 antibodies. This revealed that hypotonic low-chloride stimulation enhanced phosphorylation of NKCC2 at Ser91, Thr100 and Thr105 by twofold to threefold (Fig. 4C). No phosphorylation of Ser130 was detected in these experiments.

A docking interaction between NKCC2 and SPAK-OSR1 modulates NKCC2 phosphorylation

Inspection of the NKCC2 amino acid sequence revealed that it possesses a single highly conserved optimal motif for binding to the SPAK-OSR1 CCT-domain (RFQV, residues 20–23). In human NKCC2 there are two further motifs (KFGW, residues 176–179, and KFRI, residues 965–968) that bear similarity to the RFX[V/I] motif. To determine whether NKCC2 interacted with SPAK-OSR1 through these motifs, we overexpressed wild-type or mutant NKCC2 isoform F, in which Arg20, Lys176 or Lys965 were individually mutated to Ala, and investigated how this affected binding to endogenous SPAK-OSR1. In co-immunoprecipitation experiments we observed that wild-type NKCC2, as well as NKCC2(K176A) and NKCC2(K965A), interacted with endogenous SPAK-OSR1 (Fig. 5A). However, the NKCC2(R20A) mutant, despite being expressed at the same levels as wild-type NKCC2, failed to interact with endogenous SPAK-OSR1 (Fig. 5A).

We next utilised stable cell lines expressing either wild-type NKCC2 or the mutant NKCC2(R20A) isoform F to investigate how mutation of the motif responsible for docking to SPAK-OSR1 affected the phosphorylation of NKCC2 induced by hypotonic low-chloride treatment. This revealed that the Arg20 to Ala mutation decreased phosphorylation of NKCC2 at Thr100 and Thr105 by ~70% (Fig. 5B). Although SPAK-OSR1 did not directly phosphorylate Ser91 in vitro, we also observed that the Arg20 to Ala mutation decreased Ser91 phosphorylation by a similar extent to that at the Thr100 and Thr105 sites (Fig. 5B). By contrast, phosphorylation of Ser130 was not affected by the Arg20 to Ala mutation, further suggesting that phosphorylation of this residue is not regulated by SPAK-OSR1 (Fig. 5B).

Relative activity of NKCC2 isoforms in HEK-293 cells

We found that all three NKCC2 isoforms (F, A and B) were expressed at similar levels in HEK-293 cells following transient transfection. All isoforms interacted similarly with endogenous SPAK-OSR1, and this interaction was not significantly affected by stimulation of cells with hypotonic low-chloride conditions (Fig. 6). Hypotonic low-chloride conditions induced marked phosphorylation of all isoforms of NKCC2 at Ser91, Thr100, Thr105 and Ser130 (Fig. 6). The relative level of phosphorylation of Ser91 and Ser130 following hypotonic low-chloride stimulation was similar in all three NKCC2 isoforms (Fig. 6). By contrast, phosphorylation of Thr100 and Thr105 was fivefold to sixfold higher in isoform A and isoform B compared with isoform F (Fig. 6).

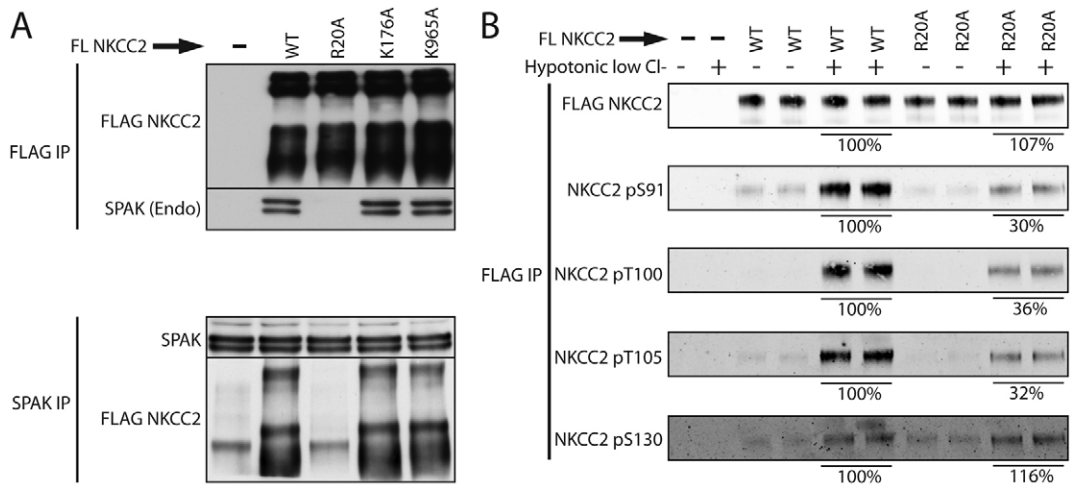

Fig. 5. The SPAK-OSR1 interaction with NKCC2 mediates NKCC2 phosphorylation. (**A**) HEK-293 cells were transfected with constructs encoding the wild-type (WT) or the indicated mutants of human FLAG–NKCC2 (isoform F) and at 36 hours post-transfection cells were lysed. FLAG–NKCC2 and endogenous SPAK were immunoprecipitated (IP), and the immunoprecipitates were subjected to immunoblot analysis for the indicated proteins. Similar results were obtained in two separate experiments. (**B**) Stably transfected HEK-293 T-Rex cell lines were induced to express wild-type or the indicated mutant form of human FLAG–NKCC2 (isoform F). At 24 hours post-induction, cells were treated with either basic (–) or hypotonic low-chloride medium (+) for 30 minutes and lysed. FLAG–NKCC2 was immunoprecipitated and quantitative immunoblotting was performed for the indicated proteins by employing the LI-COR Odyssey imaging system. Total levels of NKCC2 and NKCC2(R20A) were normalised and the level of phosphorylation of the NKCC2(R20A) mutant under hypotonic low-chloride conditions is presented as a percentage of the level of phosphorylation of wild-type NKCC2 under the same conditions. Results of duplicate samples are shown, and similar results were obtained in two separate experiments.

In order to compare the activity of different NKCC2 isoforms, we measured bumetanide-sensitive uptake of ^{86}Rb in HEK-293 cells overexpressing these enzymes at similar levels. Assays were performed in the presence of ouabain to inhibit the activity of the Na^+/K^+-ATPase, employing a similar approach to that described in a recent study (Hannemann et al., 2009). In cells not transfected with NKCC2, a low level of bumetanide-sensitive ^{86}Rb uptake was observed, which was increased approximately threefold by hypotonic low-chloride stimulation of cells, presumably owing to activation of the endogenous NKCC1 that is expressed in these

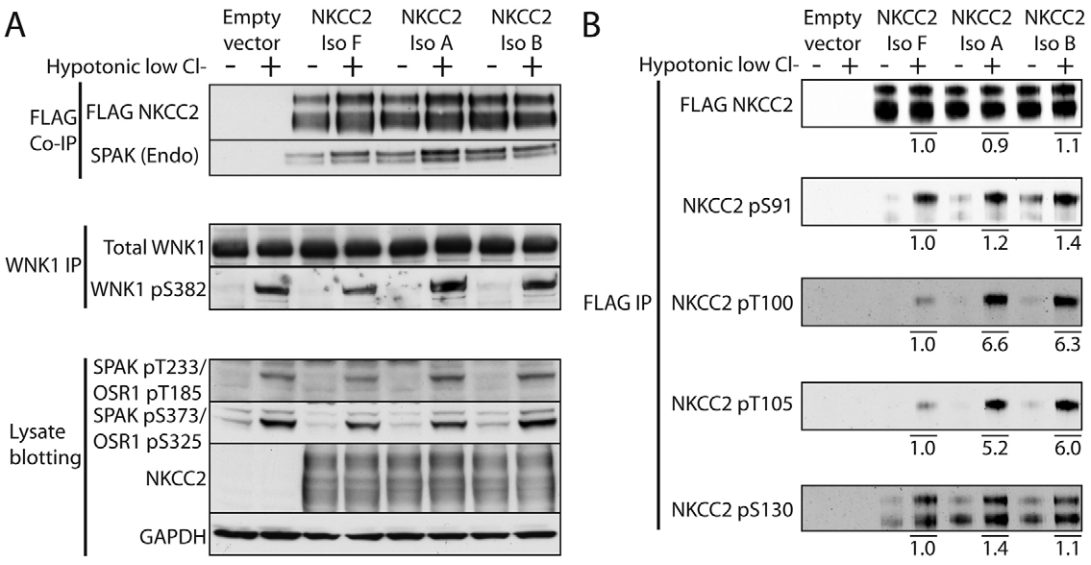

Fig. 6. Comparison of NKCC2 isoform F, isoform A and isoform B phosphorylation. (**A**) HEK-293 cells were transfected with constructs encoding the indicated wild-type forms of human NKCC2 (isoform F, isoform A or isoform B). At 36 hours post-transfection, cells were treated with either basic (–) or hypotonic low-chloride medium (+) for 30 minutes and lysed. FLAG–NKCC2 was immunoprecipitated (IP) and the immunoprecipitates were subjected to immunoblot analysis for the indicated proteins. Endogenous WNK1 was immunoprecipitated and immunoblotted for the indicated proteins. Total cell lysates were also immunoblotted for the indicated proteins. (**B**) FLAG–NKCC2 was immunoprecipitated and quantitative immunoblotting was performed for the indicated proteins by employing the LI-COR Odyssey imaging system. The total levels of NKCC2 isoform F, isoform A and isoform B were normalised and the phosphorylation level of NKCC2 isoform A and isoform B under hypotonic low-chloride conditions is presented relative to that of the NKCC2 isoform F under the same conditions.

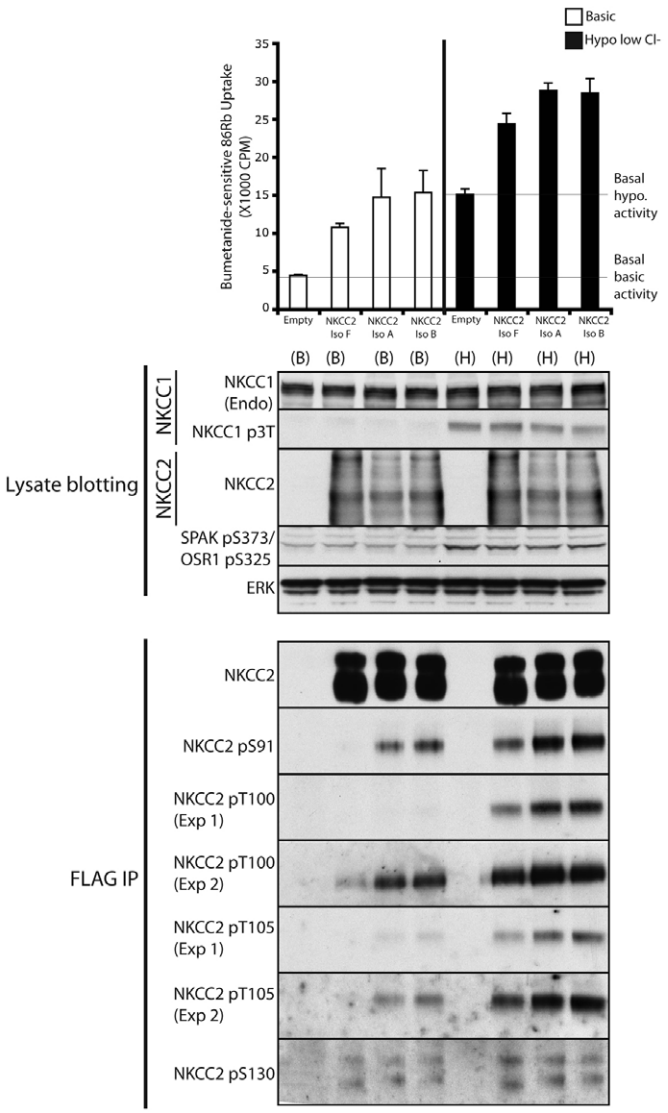

Fig. 7. Analysis of NKCC2-mediated ^{86}Rb uptake of NKCC2 isoforms (F, A and B) in HEK-293 cells. HEK-293 cells were transfected with pCMV5 empty vector or constructs encoding the indicated wild-type forms of human NKCC2 (isoform F, isoform A or isoform B). At 36 hours post-transfection, ^{86}Rb uptake was assessed in control basic (B) or hypotonic low-chloride (H) conditions in the absence or presence of 0.1 mM bumetanide in the uptake medium as described in the Materials and Methods section. For each transfection construct, the bumetanide-sensitive ^{86}Rb uptake (i.e. with the bumetanide-insensitive counts subtracted) is plotted for both basic and hypotonic low-chloride conditions. The results are presented as the mean ^{86}Rb uptake (±s.d.) for triplicate samples (top panel). Expression and phosphorylation of endogenous (Endo) NKCC1 (middle panel) and transfected NKCC2 (bottom panel) proteins were monitored in parallel experiments following immunoblot analysis for the indicated proteins. NKCC2 phosphorylation was analysed following immunoprecipitation (IP) of FLAG–NKCC2. Similar results were obtained in three separate experiments.

cells (Fig. 7, top panel). Hypotonic low-chloride conditions induced similar phosphorylation of SPAK and OSR1 at Ser373 and Ser325, respectively (the WNK1 phosphorylation site), as well as in NKCC1 in all cells (Fig. 7, middle panel). We found that cells expressing NKCC2 isoforms displayed a twofold (isoform F) or threefold (isoform A and B) higher basal activity compared with that of cells not expressing NKCC2 (Fig. 7, upper panel). Following hypotonic low-chloride stimulation, taking into consideration the contribution of the increased background NKCC1 activity, no significant further activation of NKCC2 activity was observed, despite increased phosphorylation of NKCC2 (Fig. 7, top and bottom panels).

The important role of Thr105 and Ser130 in controlling NKCC2 activity

To study the importance of the identified NKCC2 phosphorylation sites, these residues were mutated individually or in combination, and the effect that this had on NKCC2 activity under basic and hypotonic low-chloride conditions was assessed (Fig. 8A). NKCC2 isoform B was selected for this functional analysis of NKCC2 activity as this isoform proved to be more active than NKCC2 isoform F in the functional comparison studies (Fig. 7, top panel). We calculated that bumetanide inhibited NKCC2 isoform B in HEK-293 cells with an IC_{50} value of 0.54 μM (supplementary material Fig. S4), broadly consistent with previously reported values obtained employing *Xenopus laevis* oocytes as an heterologous expression system (Carota et al., 2010; Paredes et al., 2006; Plata et al., 2002). Individual mutation of Ser91, Thr95 or Thr100 did not significantly affect NKCC2 activity (Fig. 8A). Mutation of either Thr105 or Ser130 reduced NKCC2 activity by 30–40% under both treatment conditions, whereas combined mutation of the five identified phosphorylation sites completely abolished NKCC2 activity (Fig. 8A). This latter observation also confirms that the activity we are measuring is indeed attributable to NKCC2, rather than to endogenous NKCC1. We also observed that combined mutation of Thr105 and Ser130 almost abolished NKCC2 activity (Fig. 8B).

Comparison of NCC and NKCC2 localisation and phosphorylation

Previous work has suggested that the WNK-signalling pathway promotes NCC activation by stimulating plasma membrane localisation (Yang et al., 2007). We therefore compared the plasma membrane localisation of stably expressed FLAG–NCC and FLAG–NKCC2 isoform B in HEK-293 cells under basic and hypotonic low-chloride conditions (Fig. 9A,D). We found that hypotonic low-chloride stimulation markedly enhanced the plasma membrane localisation of NCC, as assessed by immunohistochemical analysis (Fig. 9B) or in isolated plasma membrane fractions (Fig. 9C). Importantly, mutation of the key activating SPAK-OSR1 Thr60 phosphorylation site on NCC, which is mutated in patients with Gitleman's syndrome, prevented hypotonic low-chloride-induced membrane translocation of NCC (Fig. 9B,C). By employing a NCC Thr60-phosphorylation-specific antibody, we observed that the phosphorylated form of NCC was localised at the plasma membrane (Fig. 9B,C). In contrast with NCC, we observed a significant amount of plasma-membrane-localised NKCC2 under basic conditions, which was not further increased by hypotonic low-chloride treatment of the cells (Fig. 9E,F). This observation might explain the observed high basal activity of NKCC2 isoforms, which is not further simulated by hypotonic low-chloride conditions (Fig. 7, top panel). Although the NKCC2 Thr105-phosphorylation-specific antibody (equivalent to Thr60 in human NCC) did not prove sensitive enough to detect phosphorylated NKCC2 in cell lines stably expressing NKCC2, we were able to detect NKCC2 Thr105 phosphorylation by employing transient transfection approaches (supplementary

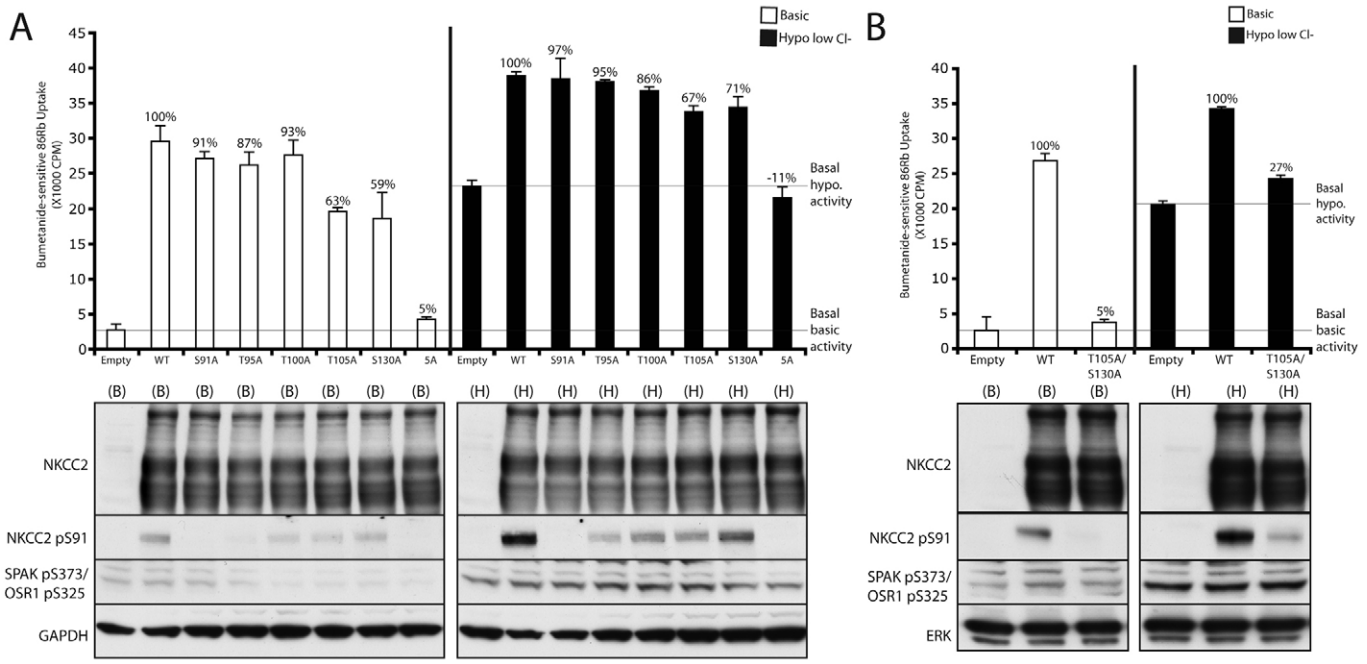

Fig. 8. Combined mutation of Thr105 and Ser130 of NKCC2 significantly inhibits NKCC2-mediated ^{86}Rb uptake in HEK-293 cells. (**A**) HEK-293 cells were transfected with pCMV5 empty vector or constructs encoding the indicated wild-type (WT) or mutant forms of human NKCC2 (isoform B) and an ^{86}Rb-uptake assay was performed as described in Fig. 7. The ^{86}Rb uptake above the basal pCMV5 empty uptake represents NKCC2-mediated ^{86}Rb-uptake activity and is set at 100% for both basic (B) and hypotonic low-chloride (H) conditions. The uptake activity of the mutant forms of NKCC2 is presented as a percentage of the wild-type NKCC2 activity. Control immunoblotting for the indicated proteins was performed in parallel. Similar results were obtained in three separate experiments. 5A corresponds to a quintuple NKCC2 mutant in which Ser91, Thr95, Thr100, Thr105 and Ser130 are replaced with Ala. (**B**) An experiment, as described in A, for the human NKCC2 (isoform B) T105A and S130A double-mutant. Similar results were obtained in three separate experiments.

material Fig. S5). NKCC2 phosphorylated at Thr105 was detected at the plasma membrane under both basic and hypotonic low-chloride conditions (supplementary material Fig. S5), consistent with the notion that it is constitutively localised at the plasma membrane. Combined mutation of Thr105 and Ser130, which renders NKCC2 functionally defective (Fig. 8B), did not affect association of NKCC2 with the plasma membrane (Fig. 9E,F). We also mutated all five identified phosphorylation sites on NKCC2 and found that this also did not inhibit the membrane localisation of NKCC2 (supplementary material Fig. S5).

Discussion

Sequence alignments of the N-terminal region of NKCC1, NKCC2 and NCC suggest that there are seven conserved regions of phosphorylation, which we have termed sites 1 to 7 (Fig. 1A). The human NKCC2 phosphorylation sites characterised in this study correspond to Ser91 (site 1), Thr95 (site 2), Thr100 (site 3), Thr105 (site 4) and Ser130 (site 6). We did not observe phosphorylation of NKCC2 at site 5 (human Thr118), corresponding to Ser73 of human NCC (Moriguchi et al., 2005), although we cannot rule out the possibility that this residue was phosphorylated at too low a stoichiometry to detect. It should be noted that we also failed to observe phosphorylation of site 5 on NCC in a previous study (Richardson et al., 2008), despite reports that phosphorylation of NCC at Ser73 is stimulated by conditions in which the WNK pathway is activated (Chiga et al., 2008; Talati et al., 2010; Yang et al., 2007). Site 5 on NKCC1 (human Thr230) is phosphorylated in response to forskolin treatment (Darman and Forbush, 2002), but the kinase mediating this and whether it is controlled by the WNK pathway have not been determined. It might be of interest to evaluate whether forskolin induces phosphorylation of NKCC2 at site 5 (human Thr118). Site 7 on NKCC2 corresponds to Ser91 of human NCC (Richardson et al., 2008) and is an acidic residue on both NKCC2 (human Glu136) and NKCC1 (human Asp248). In NCC, Ser91 phosphorylation appears to be regulated indirectly by SPAK-OSR1 as this residue is not phosphorylated by SPAK-OSR1 in vitro; however, in cells, ablation of the RFXI SPAK-OSR1-docking site impaired phosphorylation of NCC at Ser91 (Richardson et al., 2008). Moreover, in knock-in mice lacking SPAK activity, phosphorylation of NCC at Ser91 was inhibited (Rafiqi et al., 2010).

Our data suggest that three of the five identified NKCC2 phosphorylation sites (sites 2, 3 and 4; Thr95, Thr100 and Thr105, respectively) are directly phosphorylated by SPAK-OSR1 in vitro (supplementary material Fig. S1, Fig. S2 and Fig. S3B). SPAK-OSR1 also directly phosphorylates three residues in NKCC1 (sites 1, 2 and 3; Thr203, Thr207 and Thr212, respectively) (Vitari et al., 2006) and three residues in NCC (sites 1, 3 and 4; Thr46, Thr55 and Thr60, respectively) (Richardson et al., 2008). It cannot be ruled out that site 4 in NKCC1 (human Thr217) and site 2 in NCC (human Thr50) are also phosphorylated by SPAK-OSR1, but that this phosphorylation was not observed owing to low stoichiometry of phosphorylation or other technical reasons. Although we were unable to demonstrate that site 1 (Ser91) in NKCC2 was phosphorylated directly by SPAK-OSR1 in vitro, our findings in cells point towards phosphorylation of this residue being dependent upon SPAK-OSR1, as ablation of the RFQV docking site decreased

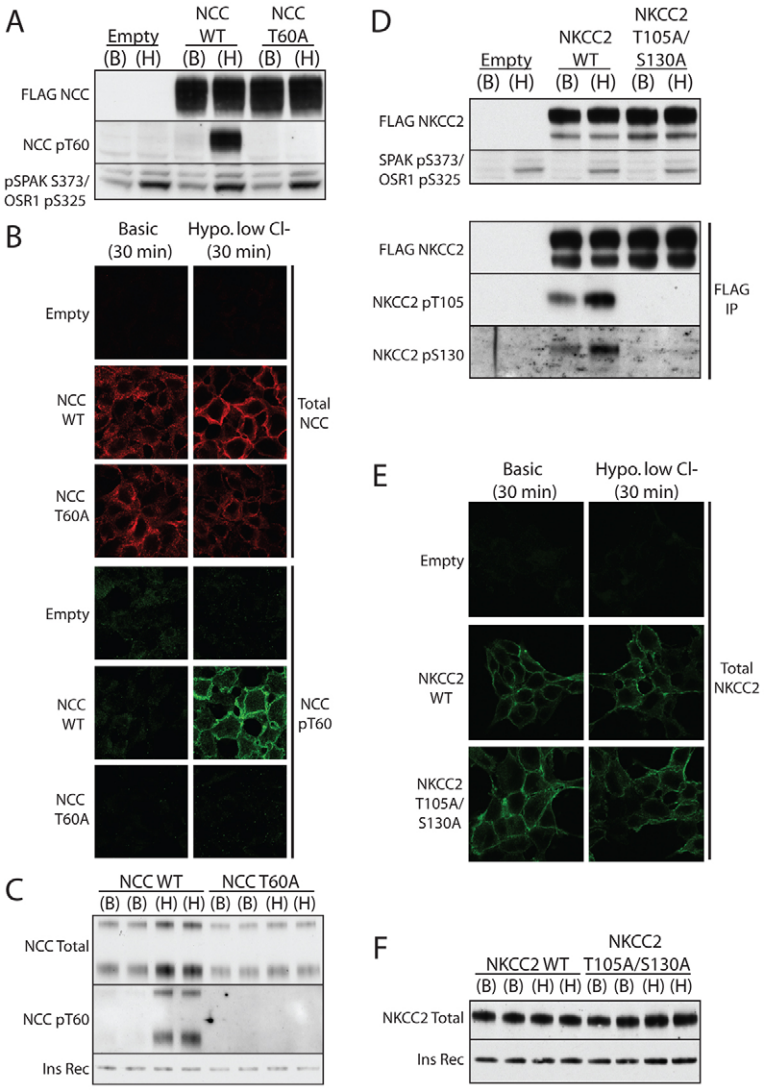

Fig. 9. Phosphorylation on Thr60 induces NCC translocation to the plasma membrane. (**A**) Stably transfected HEK-293 T-Rex cell lines were induced to express either wild-type (WT) or the indicated mutant form of human FLAG–NCC. At 24 hours post-induction, cells were treated with either basic (B) or hypotonic low-chloride buffer (H) for 30 minutes and lysed. Total cell extracts were immunoblotted for the indicated proteins. (**B**) An experiment as described in A, except that following buffer treatment cells were fixed in 4% paraformaldehyde. The cells were subsequently permeabilised and immunostained with either anti-FLAG (Total NCC) followed by Alexa-Fluor-594-labelled anti-(mouse IgG) antibody or anti-NCC phosphorylated Thr60 antibody followed by Alexa-Fluor-488-labelled anti-(sheep IgG) antibody (NCC pT60). Fluorescence imaging was performed on a laser scanning confocal microscope and the cells shown are representative of images obtained in two separate experiments. (**C**) An experiment as described in A, except that following buffer treatment cells were harvested in PBS and used to generate plasma membrane fractions as described in the Materials and Methods section. Plasma membrane fractions were immunoblotted for the indicated proteins; the levels of insulin receptor (Ins Rec) were used to normalise protein loading. Similar results were obtained in two separate experiments. (**D**) An experiment as described in A, except that stably transfected HEK-293 T-Rex cell lines expressing FLAG–NKCC2 (isoform B) were employed. NKCC2 Thr105 and Ser130 phosphorylation was monitored by immunoblotting following immunoprecipitation of FLAG–NKCC2. (**E**) An experiment as described in B. Cells were immunostained with anti-FLAG antibody (Total NKCC2) followed by Alexa-Fluor-488-labelled anti-(mouse IgG) antibody. Cells shown are representative of images obtained in three separate experiments. (**F**) An experiment as described in C for the human NKCC2 (isoform B) T105A and S130A double-mutant. Similar results were obtained in two separate experiments.

Ser91 phosphorylation to an extent similar to that of Thr100 and Thr105 phosphorylation (Fig. 5B). It is possible that the recombinant NKCC2 fragment employed might not adopt the proper conformation required for efficient phosphorylation of Ser91. It cannot be ruled out that SPAK-OSR1 might indirectly regulate phosphorylation of this residue by activating another kinase or inactivating a phosphatase that controls Ser91 phosphorylation in cells. It should also be noted that sites 1 to 4 are all Thr residues in NCC and NKCC1, but site 1 in NKCC2 (human Ser91) is a Ser residue (Fig. 1A). To our knowledge, all in vitro SPAK-OSR1 substrates analysed to date have been phosphorylated on Thr residues, perhaps suggesting that SPAK-OSR1 has a preference for phosphorylating Thr residues over Ser residues. It would be interesting to investigate how changing the phosphorylation sites on known substrates to Ser affected phosphorylation by SPAK and OSR1.

Our results indicate that Ser130 (site 6) is not controlled by SPAK or OSR1, as these kinases do not phosphorylate Ser130 in vitro (supplementary material Fig. S1, Fig. S2 and Fig. S3B). Furthermore, ablation of the RFQV docking site on NKCC2 did not inhibit Ser130 phosphorylation under conditions where phosphorylation of other SPAK/OSR1 residues were suppressed (Fig. 5B). Previous work has suggested that AMPK could phosphorylate Ser130 (Cook et al., 2009; Fraser et al., 2007), and our data with phenformin stimulation and the non-selective AMPK-inhibitor termed compound C support this conclusion (Fig. 3C and supplementary material Fig. S3). However, our data suggest that under hypotonic low-chloride conditions a distinct protein kinase phosphorylates NKCC2 at Ser130, as these conditions do not trigger significant activation of AMPK yet lead to an increased phosphorylation of NKCC2 at Ser130 (Fig. 3C). In future work it would be interesting to generate mice that lack both of the AMPK catalytic subunits in the kidney and study how this effects NKCC2 phosphorylation as well as blood pressure. We are unaware of any evidence suggesting that the equivalent Ser130 (site 6) residue on NKCC1 (human Ser242) or NCC (human Thr85) is phosphorylated.

Our findings also suggest that NKCC2 isoforms are differentially phosphorylated by SPAK-OSR1, as isoform A and B were phosphorylated at Thr100 and Thr105 to a significantly greater extent than isoform F (Figs 6 and 7, bottom panel). These observations could account for the higher basal activity of isoform A and B compared with isoform F, when assessed in HEK-293 ^{86}Rb-uptake assays (Fig. 7, top panel). These observations are consistent with previous reports that also concluded that isoforms

A and B were more active than isoform F when expressed in mammalian cells (Hannemann et al., 2009) or in *Xenopus laevis* oocytes (Gimenez et al., 2002; Plata et al., 2002). The only differences in the three isoforms of NKCC2 lie in an alternatively spliced exon encoding the proposed second transmembrane domain and a portion of the adjacent first intracellular connecting loop (Castrop and Schnermann, 2008) (Fig. 1B). It has been proposed that the higher affinity NKCC2 isoforms A and B have functionally evolved to reabsorb salt as the urine becomes more hypotonic in the cortical thick ascending limb of the loop of Henle, a region where the NKCC2 isoform F is not expressed (Gimenez et al., 2002; Plata et al., 2002). In contrast with previous work in *Xenopus laevis* oocytes (Ponce-Coria et al., 2008), we found that although hypotonic low-chloride conditions markedly enhanced phosphorylation of NKCC2, this was not accompanied by any significant increase in NKCC2 activity as judged in our cell-based ^{86}Rb-uptake assay (Fig. 7, upper panel). Another recent study also reported that NKCC2 expressed in mammalian cells was not activated upon exposure to hypotonic low-chloride conditions (Hannemann et al., 2009). These differences might suggest that the *Xenopus laevis* oocyte expression system may be optimal for studying NKCC2 activation.

When comparing NCC and NKCC2, renal ion cotransporters that are both phosphorylated by SPAK-OSR1 at equivalent residues, there are some considerable differences. First, NCC is largely dephosphorylated and inactive when expressed in cells, and hypotonic low-chloride conditions promote marked phosphorylation and activation of NCC (Richardson et al., 2008). By contrast, NKCC2 is partially phosphorylated and active when analysed under both basic conditions and hypotonic low-chloride conditions, although promoting further phosphorylation of NKCC2 does not significantly stimulate increased activity (Fig. 7, bottom and top panels). Second, we find that hypotonic low-chloride conditions promoted marked translocation of NCC to the plasma membrane. We also observed that the phosphorylated form of NCC was largely localised at the plasma membrane (Fig. 9B,C). Strikingly, mutation of the key Thr60 SPAK-OSR1 phosphorylation site inhibited the translocation of NCC to the plasma membrane induced by hypotonic low-chloride conditions (Fig. 9B,C). This is consistent with the idea that phosphorylation of Thr60 is a key trigger for membrane translocation of NCC, hence leading to enhanced salt transport. These results are also consistent with other studies reporting that the WNK pathway regulates the membrane localisation of NCC (Cai et al., 2006; Golbang et al., 2005; Wilson et al., 2003). By contrast, we have no evidence that the SPAK-OSR1 pathway controls the membrane localisation of NKCC2, as hypotonic low-chloride conditions or mutation of the identified key phosphorylation sites on NKCC2 failed to influence plasma membrane localisation (Fig. 9E,F). In line with this observation, a previous study has reported that functionally inactive Bartter Syndrome Type I mutants of NKCC2 are also routed normally to the plasma membrane when expressed in *Xenopus laevis* oocytes (Starremans et al., 2003). Nevertheless, it is important to note that it has been reported that the anti-diuretic hormone vasopressin induces phosphorylation and membrane trafficking of NKCC2 to the apical membrane of the thick ascending limb in vivo, suggesting that, under certain stimulation conditions, NKCC2 traffics to the plasma membrane in response to phosphorylation (Gimenez and Forbush, 2003). In future work it would also be important to study membrane localisation of endogenous NCC and NKCC2 in animal kidneys and verify how this is affected by knockout of SPAK and OSR1 expression or activity.

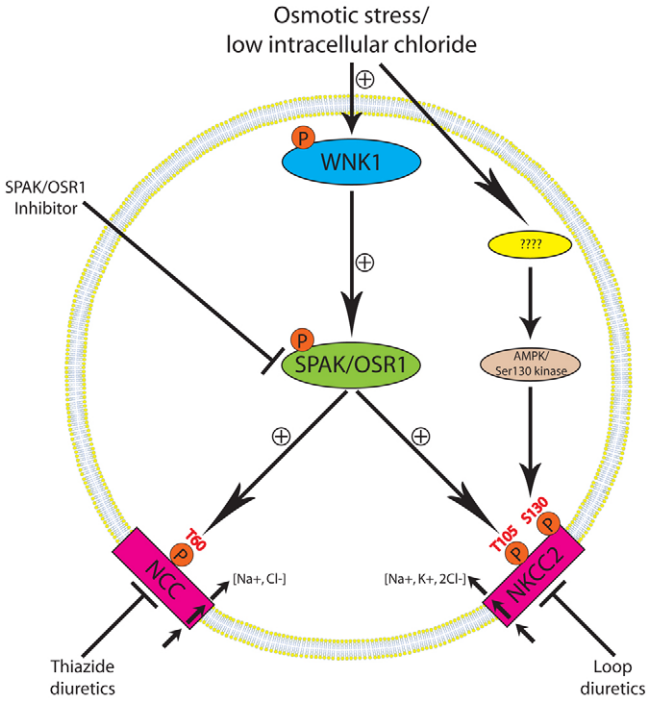

Fig. 10. Proposed mechanism of NKCC2 regulation. The WNK-SPAK-OSR1 signalling pathway and an additional signalling pathway, possibly through AMPK, regulate NKCC2 activity. Inhibitors of SPAK-OSR1 would be predicted to be effective agents at reducing blood pressure by suppressing activity of both NCC and NKCC2.

Our functional studies suggest that phosphorylation of Thr105 and Ser130 of NKCC2 is important for controlling NKCC2 activity (Fig. 8). Individual mutations of Thr105 and Ser130, but not other residues, reduced NKCC2 activity 30–40%, broadly in agreement with previous studies that analysed NKCC2 activity in *Xenopus laevis* oocytes (Fraser et al., 2007; Gimenez and Forbush, 2005; Ponce-Coria et al., 2008). Our study is the first to demonstrate that combined mutation of Thr105 and Ser130 virtually abolishes NKCC2 activity (Fig. 8B). These results contrast with the regulation of NCC and NKCC1, where the mutation of a single residue in NCC (human Thr60) (Pacheco-Alvarez et al., 2006; Richardson et al., 2008) or NKCC1 (human Thr217) (Darman and Forbush, 2002; Gagnon et al., 2007) abolishes activity.

In conclusion, our results indicate that NKCC2 is controlled through two distinct pathways, namely the WNK-SPAK-OSR1 pathway, regulating Thr105 phosphorylation, and a further pathway regulating Ser130 phosphorylation, where significant evidence points towards AMPK playing an important role (Fig. 10). NKCC2 is quantitatively responsible for ~25% of the overall renal salt re-absorption, substantially more than NCC (Gamba, 2005; O'Shaughnessy and Karet, 2006). It is therefore possible that regulation of NKCC2 function, through the presence of multiple isoforms and two signalling pathways rather than just one, provides greater versatility for fine-tuning the activity of this important ion cotransporter. Our work provides further evidence that inhibitors of SPAK-OSR1 could have therapeutic potential for the treatment of hypertension, which would work by inhibiting renal salt re-

absorption through suppressing activity of both NKCC2 and NCC. Such drugs might reduce blood pressure more efficiently than thiazide and loop diuretics, which only suppress activity of individual ion cotransporters.

Materials and Methods

Cell culture, stable cell line generation, transfections and stimulations

Human embryonic kidney HEK-293 cells were cultured on 10-cm-diameter dishes in DMEM supplemented with 10% (v/v) fetal bovine serum, 2 mM L-glutamine, 100 units/ml penicillin and 0.1 mg/ml streptomycin. HEK-293 T-Rex stably transfected cell lines were generated using the Flp-in T-REX system from Invitrogen according to the manufacturer's instructions. These stable cell lines were selected/cultured in the presence of 15 μg/ml blasticidin and 100 μg/ml hygromycin. Protein expression was induced for 24 hours with 0.1 μg/ml tetracycline. For HEK-293 transfection experiments, each dish of adherent HEK-293 cells was transfected for a period of 36 hours with 20 μl of 1 mg/ml polyethylenimine (Polysciences) and 5–10 μg of plasmid DNA, as described previously (Durocher et al., 2002). HEK-293 T-Rex stable cell lines or transfected HEK-293 cells were stimulated with either control basic or hypotonic low-chloride medium for 30 minutes (for details of the buffers, see the supplementary Materials and Methods section). Cells were lysed in 0.3 ml of ice-cold lysis buffer per dish, lysates were clarified by centrifugation at 26,000 ***g*** for 15 minutes at 4°C and the supernatants were frozen in aliquots in liquid nitrogen and stored at –20°C. Protein concentrations were determined using the Bradford method.

Composition of control and hypotonic low-chloride buffers

Basic buffer [135 mM NaCl, 5 mM KCl, 0.5 mM $CaCl_2$, 0.5 mM $MgCl_2$, 0.5 mM Na_2HPO_4, 0.5mM Na_2SO_4 and 15 mM HEPES (pH 7.5)]. Hypotonic low chloride buffer [67.5 mM Na-gluconate, 2.5 mM K-gluconate, 0.25 mM $CaCl_2$, 0.25 mM $MgCl_2$, 0.5 mM Na_2HPO_4, 0.5 mM Na_2SO_4 and 7.5 mM HEPES (pH 7.5)].

Immunoprecipitation of endogenous WNK1, SPAK and NKCC2

WNK1 and SPAK were immunoprecipitated from clarified HEK-293 cell lysates, whereas NKCC2 was immunoprecipitated from clarified mouse kidney extracts. Antibodies were coupled with protein-G–Sepharose at a ratio of 1 μg of antibody per 1 μl of beads. A total of 1 mg of clarified cell lysate or mouse kidney extract was incubated with 5 μg of antibody conjugated to 5 μl of protein-G–Sepharose. Incubation was for 1 hour at 4°C with gentle agitation, and the immunoprecipitates were washed three times with 1 ml of lysis buffer containing either 0.15 M NaCl (for SPAK) or 0.5 M NaCl (for WNK1 or NKCC2) and twice with 1 ml of buffer A. Bound proteins were eluted in Buffer A containing LDS sample buffer.

Affinity-purification of endogenous SPAK and OSR1 from mouse kidney employing the biotin-RFQV peptide

A total of 1 mg of clarified mouse kidney lysate was incubated with 10 μg of biotinylated RFQV-motif-containing peptide derived from WNK4 (biotin–SEEGKPQLVGRFQVTSSK) for 1 hour at 4°C with gentle agitation (Vitari et al., 2006). Then, 10 μl of streptavidin–Sepharose was subsequently added for 30 minutes at 4°C with gentle agitation. The beads were washed three times with 1 ml of lysis buffer containing 0.5 M NaCl and twice with 1 ml of buffer A. Bound proteins were eluted in Buffer A containing LDS sample buffer and subjected to immunoblot analysis.

Perfusion of mouse kidneys

All animal studies were approved by the University of Dundee Ethics Committee and performed under a UK Home Office project license. Male C57BL/6 mice (~8 weeks old) were obtained from Harlan (Bicester, UK) and received standard laboratory chow and water ad libitum. For kidney perfusion experiments, mice were terminally anaesthetised by intraperitoneal injection of pentobarbital sodium diluted in PBS (90 mg/kg of body weight). Mice were killed by cervical dislocation and the renal artery was cannulated with a blunted 23-gauge needle. Pre-warmed (~37°C) basic or hypotonic low-chloride buffer was infused for 15 minutes (~700 μl/minute) in situ by a low flow rate pump (101U/R; Watson-Marow, UK). At the end of perfusion, the kidney was removed and rapidly frozen in liquid nitrogen and stored at –80°C. Frozen kidney tissues were homogenised (Polytron homogenizer; Kinematica Polytron, Brinkmann, CT) in a tenfold mass excess of ice-cold 1% (w/v) Triton X-100 lysis buffer. Homogenates were then centrifuged for 20 minutes at 13,000 ***g*** at 4°C and the supernatant was collected. The total protein concentration was determined by the Bradford method using BSA as a standard, and lysates were snap-frozen in liquid nitrogen and stored at –80°C.

^{86}Rb-uptake assay in HEK-293 cells

HEK-293 cells were plated at a confluence of 50–60% in 12-well plates (2.4-cm-diameter per well) and transfected with wild-type or various mutant forms of full-length human NKCC2. Each well of HEK-293 cells was transfected with 2.5 μl of 1 mg/ml polyethylenimine and 1 μg of plasmid DNA. The ^{86}Rb-uptake assay was performed on the cells at 36 hours post-transfection. Culture medium was removed from the wells and replaced with either basic control or hypotonic low-chloride medium for 15 minutes. Then the medium was removed and replaced with either basic or hypotonic low-chloride medium plus 1 mM ouabain in the presence or absence of 0.1 mM bumetanide for a further 15 minutes. After this period, cells incubated in basic medium were washed twice with isotonic uptake medium containing the same additives (ouabain with or without bumetanide), with those incubated in hypotonic low-chloride medium washed in hypotonic uptake medium plus additives (ouabain with or without bumetanide). Following washing, cells were incubated with identical isotonic or hypotonic uptake medium containing 0.148–0.37 MBq/ml of ^{86}Rb for 10 minutes. After this period, cells were rapidly washed three times with ice-cold non-radioactive medium. The cells were lysed in 300 μl of ice-cold lysis buffer and ^{86}Rb-uptake quantified on a PerkinElmer liquid scintillation analyser.

Immunohistochemistry

HEK-293 T-Rex stably transfected cell lines or transiently transfected HEK-293 cells were cultured on coverslips to a confluency of 70–80%. Following stimulation with either basic control or hypotonic low-chloride buffer for 30 minutes, cells were fixed for 10 minutes with 4% (v/v) paraformaldehyde in PBS and washed twice with PBS. Cells were then permeabilised in PBS containing 0.2% Triton X-100 for 20 minutes, blocked for 30 minutes in PBS-TG [PBS containing 0.2% Tween-20 and 3% (v/v) fish-skin gelatin], incubated for 1 hour at room temperature in primary antibodies prepared in PBS-TG (the antibody against FLAG was used at 1:500 and that against NCC phosphorylated at Thr60 was used at 2 μg/ml, supplemented with the corresponding dephosphopeptide at 10 μg/ml). After washing six times in PBS-T (PBS containing 0.2% v/v Tween-20), cells were incubated for 30 minutes at room temperature in secondary antibodies prepared in PBS-TG [1:500 dilution of Alexa-Fluor-conjugated donkey anti-(mouse IgG) or donkey anti-(sheep IgG)], washed six times in PBS-T, washed once in water and mounted onto slides using hydromount. Cells were imaged on either a Zeiss LSM 510 META or a LSM 700 confocal microscope using either the ×100 alpha Plan-Fluor NA1.45 or ×100 alpha Plan-Apochromat NA1.46 objective.

Plasma membrane fractionation

A plasma membrane protein extraction kit from Biovision (number K268) was employed for the generation of plasma membrane fractions. Five dishes of HEK-293 T-Rex stably transfected cell lines at a confluency of 80–90% were employed for each plasma membrane fraction. Cells were stimulated with either basic control or hypotonic low-chloride buffer for 30 minutes, and plasma membrane fractions were prepared according to the manufacturer's guidelines. The resulting plasma membrane pellet was dissolved in 100 μl of 1% (w/v) Triton X-100 lysis buffer prior to immunoblotting.

Further experimental details

Further details on materials, general methods, antibodies, buffers, plasmids, expression and purification of FLAG–NKCC2 in HEK-293 cells, expression and purification of GST-tagged SPAK, OSR1 and NKCC2(1–174) in *E. coli*, immunoblotting, immunoprecipitation and assay of AMPKα1, assay of NKCC2 phosphorylation by SPAK and OSR1, identification of phosphorylation sites on FLAG–NKCC2 expressed in HEK-293 cells and phosphorylation site mapping are provided in the supplementary Materials and Methods section.

We acknowledge the Sequencing Service (College of Life Sciences, University of Dundee, UK) for DNA sequencing coordinated by Nicholas Helps, the Post Genomics and Molecular Interactions Centre for Mass Spectrometry facilities (College of Life Sciences, University of Dundee, UK) coordinated by Nicholas Morrice and the protein production and antibody purification teams [Division of Signal Transduction Therapy (DSTT), University of Dundee] coordinated by Hilary McLauchlan and James Hastie for generation of antibodies. We thank the Medical Research Council and the pharmaceutical companies supporting the Division of Signal Transduction Therapy Unit (AstraZeneca, Boehringer-Ingelheim, GlaxoSmithKline, Merck KgaA and Pfizer) for financial support. Deposited in PMC for release after 6 months.

Supplementary material available online at
http://jcs.biologists.org/cgi/content/full/124/5/789/DC1

Supplementary Materials and Methods available online at
http://www.lifesci.dundee.ac.uk/other/files/supplementary_text.doc

References

Anselmo, A. N., Earnest, S., Chen, W., Juang, Y. C., Kim, S. C., Zhao, Y. and Cobb, M. H. (2006). WNK1 and OSR1 regulate the Na+, K+, 2Cl- cotransporter in HeLa cells. *Proc. Natl. Acad. Sci. USA* **103**, 10883-10888.

Bain, J., Plater, L., Elliott, M., Shpiro, N., Hastie, C. J., McLauchlan, H., Klevernic, I., Arthur, J. S., Alessi, D. R. and Cohen, P. (2007). The selectivity of protein kinase inhibitors: a further update. *Biochem. J.* **408**, 297-315.

Cai, H., Cebotaru, V., Wang, Y. H., Zhang, X. M., Cebotaru, L., Guggino, S. E. and Guggino, W. B. (2006). WNK4 kinase regulates surface expression of the human sodium chloride cotransporter in mammalian cells. *Kidney Int.* **69**, 2162-2170.

Carota, I., Theilig, F., Oppermann, M., Kongsuphol, P., Rosenauer, A., Schreiber, R., Jensen, B. L., Walter, S., Kunzelmann, K. and Castrop, H. (2010) Localization and functional characterization of the human NKCC2 isoforms. *Acta Physiol. (Oxf.)* **199**, 327-338.

Castrop, H. and Schnermann, J. (2008). Isoforms of renal Na-K-2Cl cotransporter NKCC2: expression and functional significance. *Am. J. Physiol. Renal Physiol.* **295**, F859-F866.

Chiga, M., Rai, T., Yang, S. S., Ohta, A., Takizawa, T., Sasaki, S. and Uchida, S. (2008). Dietary salt regulates the phosphorylation of OSR1/SPAK kinases and the sodium chloride cotransporter through aldosterone. *Kidney Int.* **74**, 1403-1409.

Cook, N., Fraser, S. A., Katerelos, M., Katsis, F., Gleich, K., Mount, P. F., Steinberg, G. R., Levidiotis, V., Kemp, B. E. and Power, D. A. (2009). Low salt concentrations activate AMP-activated protein kinase in mouse macula densa cells. *Am. J. Physiol. Renal Physiol.* **296**, F801-F809.

Darman, R. B. and Forbush, B. (2002). A regulatory locus of phosphorylation in the N terminus of the Na-K-Cl cotransporter, NKCC1. *J. Biol. Chem.* **277**, 37542-37550.

Dowd, B. F. and Forbush, B. (2003). PASK (proline-alanine-rich STE20-related kinase), a regulatory kinase of the Na-K-Cl cotransporter (NKCC1). *J. Biol. Chem.* **278**, 27347-27353.

Durocher, Y., Perret, S. and Kamen, A. (2002). High-level and high-throughput recombinant protein production by transient transfection of suspension-growing human 293-EBNA1 cells. *Nucleic Acids Res.* **30**, E9.

Flatman, P. W. (2008). Cotransporters, WNKs and hypertension: an update. *Curr. Opin. Nephrol. Hypertens.* **17**, 186-192.

Fraser, S. A., Gimenez, I., Cook, N., Jennings, I., Katerelos, M., Katsis, F., Levidiotis, V., Kemp, B. E. and Power, D. A. (2007). Regulation of the renal-specific Na+-K+-2Cl- co-transporter NKCC2 by AMP-activated protein kinase (AMPK). *Biochem. J.* **405**, 85-93.

Gagnon, K. B., England, R. and Delpire, E. (2007). A single binding motif is required for SPAK activation of the Na-K-2Cl cotransporter. *Cell. Physiol. Biochem.* **20**, 131-142.

Gamba, G. (2005). Molecular physiology and pathophysiology of electroneutral cation-chloride cotransporters. *Physiol. Rev.* **85**, 423-493.

Gimenez, I. and Forbush, B. (2003). Short-term stimulation of the renal Na-K-Cl cotransporter (NKCC2) by vasopressin involves phosphorylation and membrane translocation of the protein. *J. Biol. Chem.* **278**, 26946-26951.

Gimenez, I. and Forbush, B. (2005). Regulatory phosphorylation sites in the NH2 terminus of the renal Na-K-Cl cotransporter (NKCC2). *Am. J. Physiol. Renal Physiol.* **289**, F1341-F1345.

Gimenez, I., Isenring, P. and Forbush, B. (2002). Spatially distributed alternative splice variants of the renal Na-K-Cl cotransporter exhibit dramatically different affinities for the transported ions. *J. Biol. Chem.* **277**, 8767-8770.

Golbang, A. P., Murthy, M., Hamad, A., Liu, C. H., Cope, G., Van't Hoff, W., Cuthbert, A. and O'Shaughnessy, K. M. (2005). A new kindred with pseudohypoaldosteronism type II and a novel mutation (564D>H) in the acidic motif of the WNK4 gene. *Hypertension* **46**, 295-300.

Hannemann, A., Christie, J. K. and Flatman, P. W. (2009). Functional expression of the Na-K-2Cl cotransporter NKCC2 in mammalian cells fails to confirm the dominant-negative effect of the AF splice variant. *J. Biol. Chem.* **284**, 35348-35358.

Lenertz, L. Y., Lee, B. H., Min, X., Xu, B. E., Wedin, K., Earnest, S., Goldsmith, E. J. and Cobb, M. H. (2005). Properties of WNK1 and implications for other family members. *J. Biol. Chem.* **280**, 26653-26658.

Lin, S. H., Shiang, J. C., Huang, C. C., Yang, S. S., Hsu, Y. J. and Cheng, C. J. (2005). Phenotype and genotype analysis in Chinese patients with Gitelman's syndrome. *J. Clin. Endocrinol. Metab.* **90**, 2500-2507.

Maki, N., Komatsuda, A., Wakui, H., Ohtani, H., Kigawa, A., Aiba, N., Hamai, K., Motegi, M., Yamaguchi, A., Imai, H. et al. (2004). Four novel mutations in the thiazide-sensitive Na-Cl co-transporter gene in Japanese patients with Gitelman's syndrome. *Nephrol. Dial. Transplant.* **19**, 1761-1766.

Moriguchi, T., Urushiyama, S., Hisamoto, N., Iemura, S., Uchida, S., Natsume, T., Matsumoto, K. and Shibuya, H. (2005). WNK1 regulates phosphorylation of cation-chloride-coupled cotransporters via the STE20-related kinases, SPAK and OSR1. *J. Biol. Chem.* **280**, 42685-42693.

O'Shaughnessy, K. M. and Karet, F. E. (2006). Salt handling and hypertension. *Annu. Rev. Nutr.* **26**, 343-365.

Pacheco-Alvarez, D., Cristobal, P. S., Meade, P., Moreno, E., Vazquez, N., Munoz, E., Diaz, A., Juarez, M. E., Gimenez, I. and Gamba, G. (2006). The Na+:Cl- cotransporter is activated and phosphorylated at the amino-terminal domain upon intracellular chloride depletion. *J. Biol. Chem.* **281**, 28755-28763.

Paredes, A., Plata, C., Rivera, M., Moreno, E., Vazquez, N., Munoz-Clares, R., Hebert, S. C. and Gamba, G. (2006). Activity of the renal Na+-K+-2Cl- cotransporter is reduced by mutagenesis of N-glycosylation sites: role for protein surface charge in Cl- transport. *Am. J. Physiol. Renal Physiol.* **290**, F1094-F1102.

Payne, J. A. and Forbush, B., III (1994). Alternatively spliced isoforms of the putative renal Na-K-Cl cotransporter are differentially distributed within the rabbit kidney. *Proc. Natl. Acad. Sci. USA* **91**, 4544-4548.

Piechotta, K., Lu, J. and Delpire, E. (2002). Cation chloride cotransporters interact with the stress-related kinases Ste20-related proline-alanine-rich kinase (SPAK) and oxidative stress response 1 (OSR1). *J. Biol. Chem.* **277**, 50812-50819.

Plata, C., Meade, P., Vazquez, N., Hebert, S. C. and Gamba, G. (2002). Functional properties of the apical Na+-K+-2Cl- cotransporter isoforms. *J. Biol. Chem.* **277**, 11004-11012.

Ponce-Coria, J., San-Cristobal, P., Kahle, K. T., Vazquez, N., Pacheco-Alvarez, D., de Los Heros, P., Juarez, P., Munoz, E., Michel, G., Bobadilla, N. A. et al. (2008). Regulation of NKCC2 by a chloride-sensing mechanism involving the WNK3 and SPAK kinases. *Proc. Natl. Acad. Sci. USA* **105**, 8458-8463.

Rafiqi, F. H., Zuber, A. M., Glover, M., Richardson, C., Fleming, S., Jovanovic, S., Jovanovic, A., O'Shaughnessy, K. M. and Alessi, D. R. (2010). Role of the WNK-activated SPAK kinase in regulating blood pressure. *EMBO Mol. Med.* **2**, 63-75.

Richardson, C. and Alessi, D. R. (2008). The regulation of salt transport and blood pressure by the WNK-SPAK/OSR1 signalling pathway. *J. Cell Sci.* **121**, 3293-3304.

Richardson, C., Rafiqi, F. H., Karlsson, H. K., Moleleki, N., Vandewalle, A., Campbell, D. G., Morrice, N. A. and Alessi, D. R. (2008). Activation of the thiazide-sensitive Na+-Cl- cotransporter by the WNK-regulated kinases SPAK and OSR1. *J. Cell Sci.* **121**, 675-684.

Shao, L., Ren, H., Wang, W., Zhang, W., Feng, X., Li, X. and Chen, N. (2008). Novel SLC12A3 mutations in Chinese patients with Gitelman's syndrome. *Nephron Physiol.* **108**, p29-36.

Simon, D. B., Karet, F. E., Hamdan, J. M., DiPietro, A., Sanjad, S. A. and Lifton, R. P. (1996a). Bartter's syndrome, hypokalaemic alkalosis with hypercalciuria, is caused by mutations in the Na-K-2Cl cotransporter NKCC2. *Nat. Genet.* **13**, 183-188.

Simon, D. B., Nelson-Williams, C., Bia, M. J., Ellison, D., Karet, F. E., Molina, A. M., Vaara, I., Iwata, F., Cushner, H. M., Koolen, M. et al. (1996b). Gitelman's variant of Bartter's syndrome, inherited hypokalaemic alkalosis, is caused by mutations in the thiazide-sensitive Na-Cl cotransporter. *Nat. Genet.* **12**, 24-30.

Starremans, P. G., Kersten, F. F., Knoers, N. V., van den Heuvel, L. P. and Bindels, R. J. (2003). Mutations in the human Na-K-2Cl cotransporter (NKCC2) identified in Bartter syndrome type I consistently result in nonfunctional transporters. *J. Am. Soc. Nephrol.* **14**, 1419-1426.

Talati, G., Ohta, A., Rai, T., Sohara, E., Naito, S., Vandewalle, A., Sasaki, S. and Uchida, S. (2010). Effect of angiotensin II on the WNK-OSR1/SPAK-NCC phosphorylation cascade in cultured mpkDCT cells and in vivo mouse kidney. *Biochem. Biophys. Res. Commun.* **393**, 844-848.

Van Huyen, J. P., Bens, M., Teulon, J. and Vandewalle, A. (2001). Vasopressin-stimulated chloride transport in transimmortalized mouse cell lines derived from the distal convoluted tubule and cortical and inner medullary collecting ducts. *Nephrol. Dial. Transplant.* **16**, 238-245.

Vitari, A. C., Deak, M., Morrice, N. A. and Alessi, D. R. (2005). The WNK1 and WNK4 protein kinases that are mutated in Gordon's hypertension syndrome phosphorylate and activate SPAK and OSR1 protein kinases. *Biochem. J.* **391**, 17-24.

Vitari, A. C., Thastrup, J., Rafiqi, F. H., Deak, M., Morrice, N. A., Karlsson, H. K. and Alessi, D. R. (2006). Functional interactions of the SPAK/OSR1 kinases with their upstream activator WNK1 and downstream substrate NKCC1. *Biochem. J.* **397**, 223-231.

Wilson, F. H., Disse-Nicodeme, S., Choate, K. A., Ishikawa, K., Nelson-Williams, C., Desitter, I., Gunel, M., Milford, D. V., Lipkin, G. W., Achard, J. M. et al. (2001). Human hypertension caused by mutations in WNK kinases. *Science* **293**, 1107-1112.

Wilson, F. H., Kahle, K. T., Sabath, E., Lalioti, M. D., Rapson, A. K., Hoover, R. S., Hebert, S. C., Gamba, G. and Lifton, R. P. (2003). Molecular pathogenesis of inherited hypertension with hyperkalemia: the Na-Cl cotransporter is inhibited by wild-type but not mutant WNK4. *Proc. Natl. Acad. Sci. USA* **100**, 680-684.

Yang, S. S., Morimoto, T., Rai, T., Chiga, M., Sohara, E., Ohno, M., Uchida, K., Lin, S. H., Moriguchi, T., Shibuya, H. et al. (2007). Molecular pathogenesis of pseudohypoaldosteronism type II: generation and analysis of a Wnk4(D561A/+) knockin mouse model. *Cell Metab.* **5**, 331-344.

Yang, T., Park, J. M., Arend, L., Huang, Y., Topaloglu, R., Pasumarthy, A., Praetorius, H., Spring, K., Briggs, J. P. and Schnermann, J. (2000). Low chloride stimulation of prostaglandin E2 release and cyclooxygenase-2 expression in a mouse macula densa cell line. *J. Biol. Chem.* **275**, 37922-37929.

Zagorska, A., Pozo-Guisado, E., Boudeau, J., Vitari, A. C., Rafiqi, F. H., Thastrup, J., Deak, M., Campbell, D. G., Morrice, N. A., Prescott, A. R. et al. (2007). Regulation of activity and localization of the WNK1 protein kinase by hyperosmotic stress. *J. Cell Biol.* **176**, 89-100.

Zhou, G., Myers, R., Li, Y., Chen, Y., Shen, X., Fenyk-Melody, J., Wu, M., Ventre, J., Doebber, T., Fujii, N. et al. (2001). Role of AMP-activated protein kinase in mechanism of metformin action. *J. Clin. Invest.* **108**, 1167-1174.